

# Comparison of Naproxen Release from Nano- and Micro-Suspensions with Its Dissolution from Untreated and Micronized Powder

K. Tsinman<sup>1</sup>, O. Tsinman<sup>1</sup>, B. Riebesehl<sup>2</sup>, and M. Juhnke<sup>2</sup>

<sup>1</sup>Pion Inc, 10 Cook Street, Billerica, MA 01821, USA; <sup>2</sup>Novartis Pharma AG, Technical R&D, P.O. Box, CH-4002 Basel, Switzerland

## INTRODUCTION

The objective of this study was to develop a method of *in situ* concentration monitoring of free API being released from a nano-suspension without a need for separation of undissolved nanoparticles. A comparison of the dissolution behavior of micronized and untreated naproxen (API) powder with the kinetics of free API release from nano- and micro-suspensions was also a goal of this work.

## MATERIALS AND METHODS

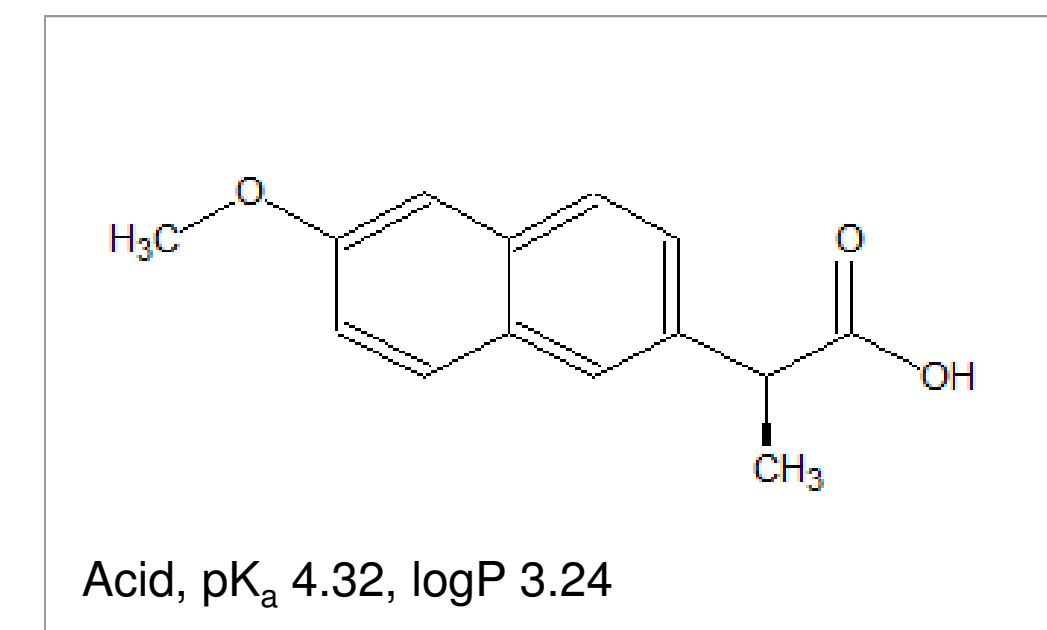


**Figure 1.** Chemical structure and physico-chemical parameters of naproxen.

Untreated powder of naproxen (Figure 1) free acid (FA-Untreated) was purchased from Sigma (St. Louis MO, USA). Micronized powder of naproxen (FA-Micronized) was obtained from Novartis AG (Basel, Switzerland). A microsuspension was prepared by suspending FA-Micronized (10% w/w) in a mixture of hydroxypropyl cellulose (HPC, type Klucel LF 2.5% w/w), sodium dodecyl sulfate (SDS, 0.05% w/w) and deionized water (87.45% w/w). A nanosuspension was prepared by further reduction of the particle size between colloid grinding media using wet media milling.

The particle size of the powders and the micro-suspension was characterized using laser light diffraction (Helos, Sympatec GmbH, Clausthal-Zellerfeld, Germany). For the nanosuspension the Brownian motion principle was used for particle size determination (Zetasizer Nano ZS, Malvern Instruments Ltd., Worcestershire, UK). Morphology of the samples was studied using scanning electron microscopy (SEM, Supra 40, Carl Zeiss SMT GmbH, Oberkochen, Germany). The dissolution behavior of naproxen powders in pH 1.2 USP buffer as well as release of free naproxen from its micro- and nanosuspensions to the buffer were monitored *in situ* using the  $\mu$ DISS Profiler (Pion, Billerica MA, USA, Figure 2).



**Figure 2.** The  $\mu$ DISS Profiler from Pion Inc monitors concentration in real time in 8 temperature controlled vessels using only 1 – 20 mL of dissolution media.

## RESULTS AND DISCUSSION

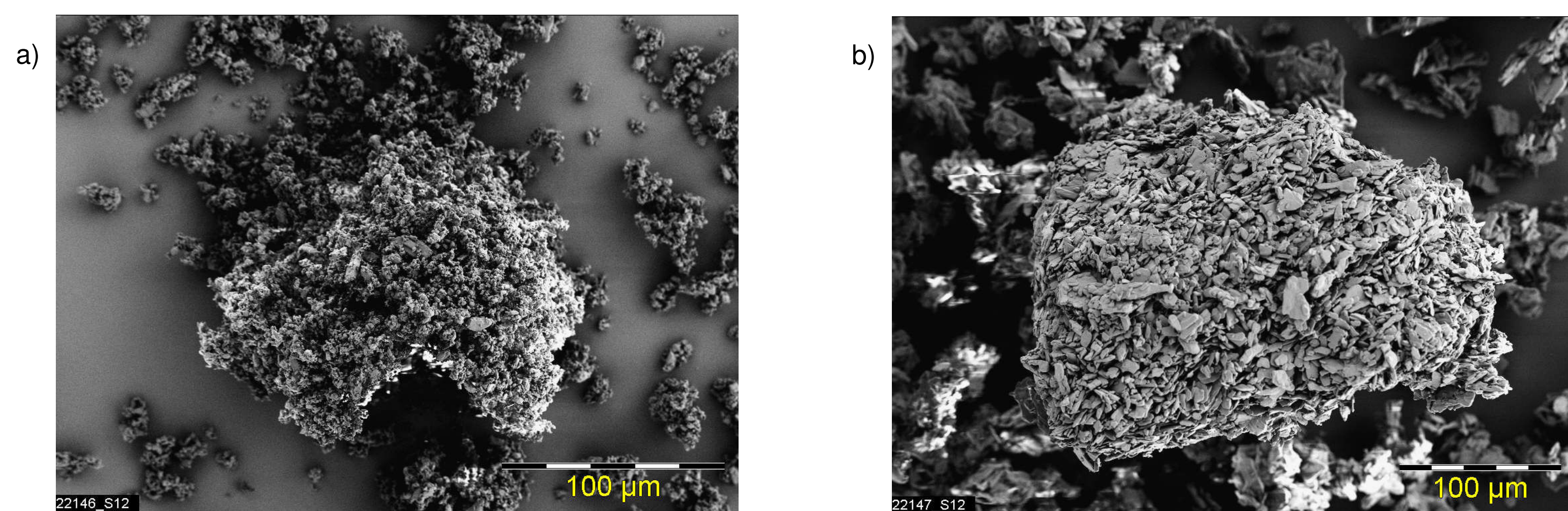
### Particle Size, Morphology and Crystallinity

**Table 1.** Particle size distribution in powders and the microsuspension.

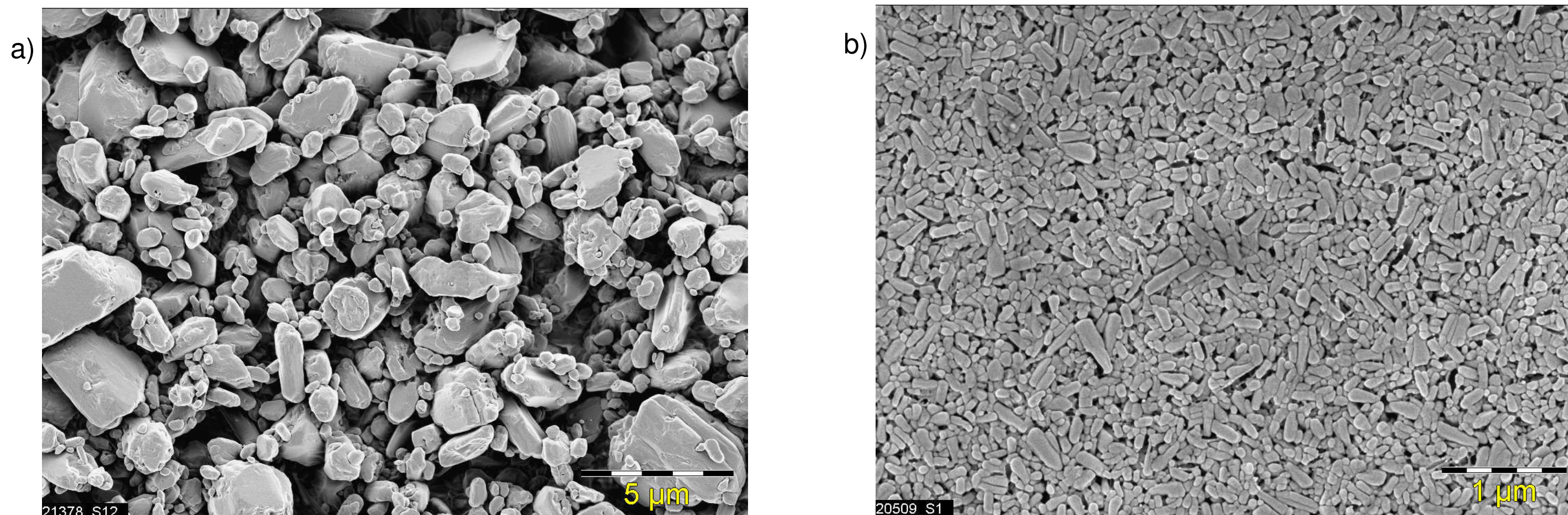
Naproxen	x <sub>10</sub> μm	x <sub>50</sub> μm	x <sub>90</sub> μm
FA-Untreated	3.2	11.9	39.6
FA-Micronized	0.9	2.6	6.1
Microsuspension	0.9	2.4	5.8

Table 1 summarizes particle sizes (volume weighted) for the untreated and micronized powders and for the microsuspension. The mean particle size in the nanosuspension was determined to be 153 nm with a polydispersity index of 0.13.

Morphology of the powders and suspensions is presented in Figure 3 and Figure 4 correspondingly.



**Figure 3.** SEM images of a) FA-Micronized and b) FA-Untreated.



**Figure 4.** SEM images of a) Naproxen Microsuspension and b) Nanosuspension.

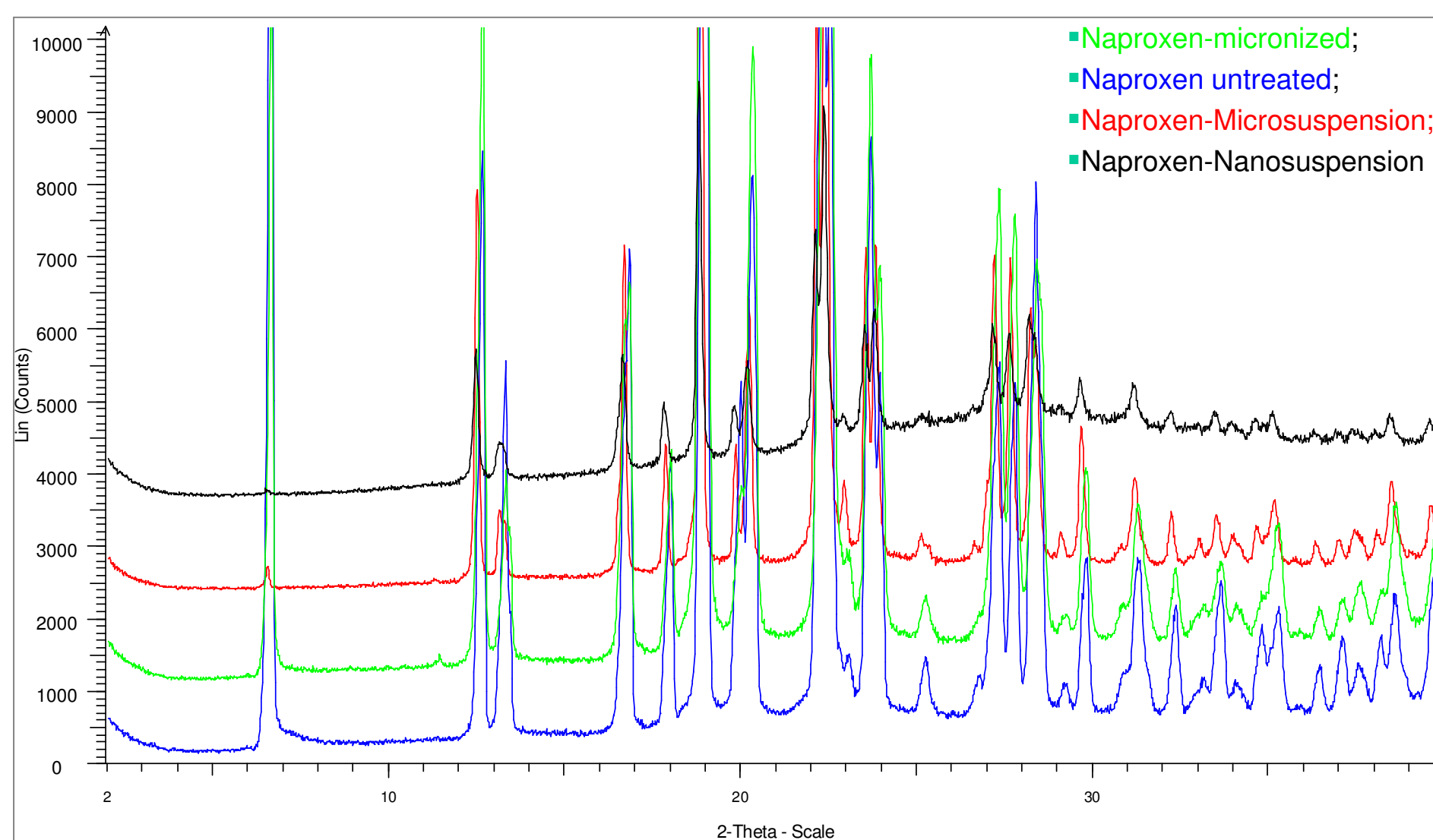


**Figure 5.** X-Ray characterization of Naproxen forms.

X-ray diffraction confirmed the same crystalline structure among all studied forms of naproxen, see Figure 5.

### Dissolution Behavior of Naproxen Powder and a Microsuspension

Dissolution experiments were conducted using the  $\mu$ DISS Profiler instrument on 10 mL of pH 1.2 USP buffer and 0.5 – 1.2 mg of Naproxen powder per vial. Although, as expected, the dissolution rate for FA-Micronized (Figure 6 a) and b)) was significantly higher than for FA-Untreated (Figures 6 c) and d)) both forms reached the same equilibrium solubility level of about 18 – 20  $\mu$ g/mL. Calculation of concentrations were performed using derivative spectroscopy to correct for the radiation scattering effects.

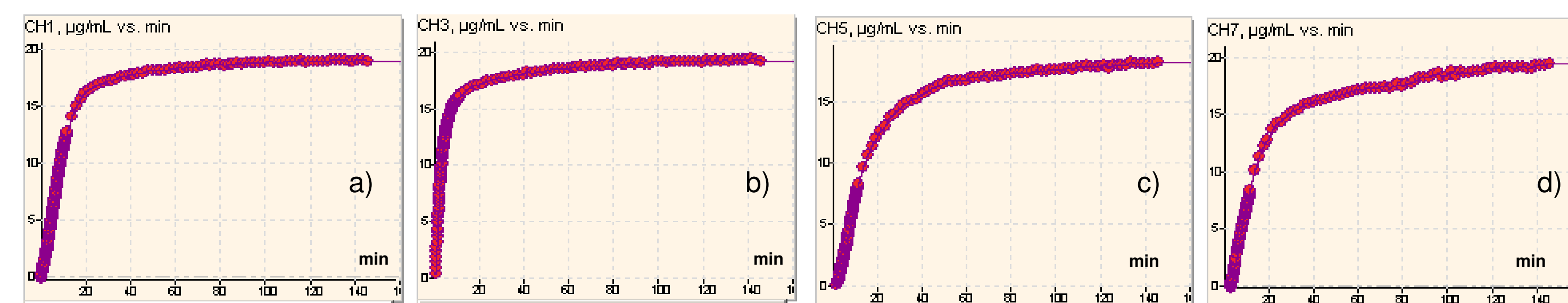


**Figure 6.** Dissolution curves ( $\mu$ g/mL versus min.) for a) 0.7 mg load and b) 1.1 mg load of FA-Micronized and c) 0.5 mg load and d) 1.1 mg load of FA-Untreated powder in 10 mL of pH 1.2 USP medium.

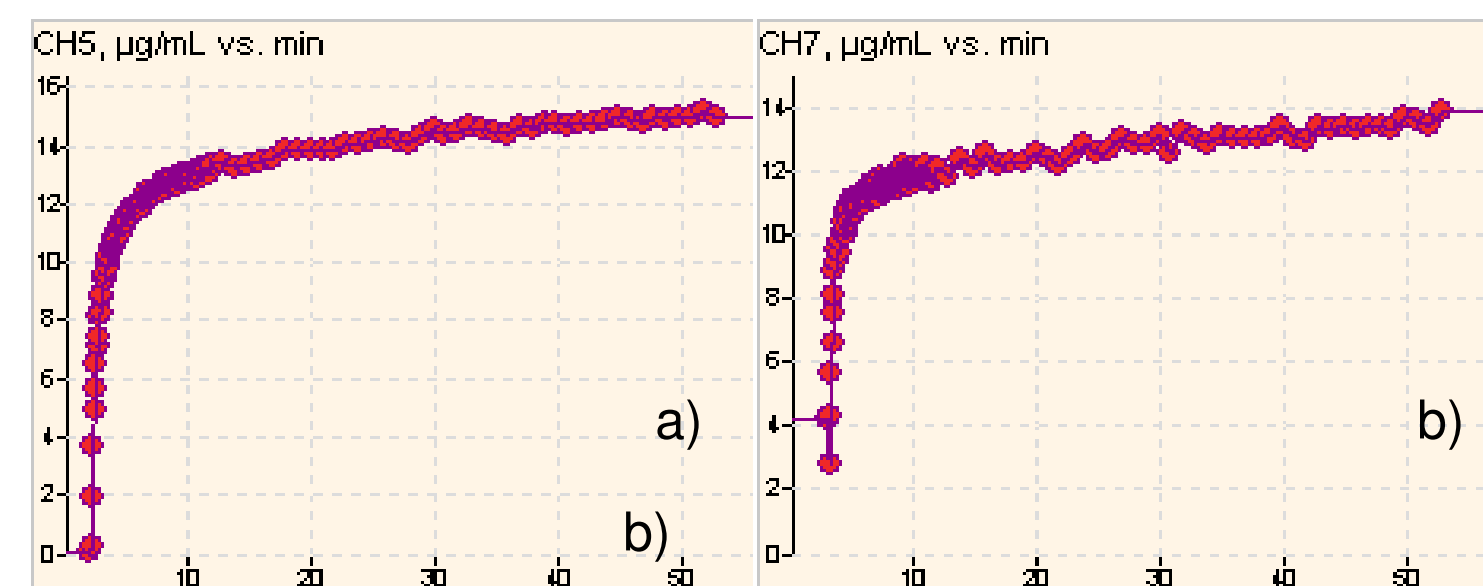


**Figure 7.** Dissolution curves ( $\mu$ g/mL versus min.) for a) 50  $\mu$ g/mL load and b) 100  $\mu$ g/mL load of naproxen microsuspension in pH 1.2 USP medium.

The release behavior of Naproxen from the microsuspension (Figure 7) was similar to its dissolution from powders. The effective specific area and corresponding “spherical” radius was calculated by fitting the dissolution curves to the model described in *Avdeef et. al. Chem. Biodev. 2009, 6 (11), 1796*. Results are presented in the Table 2 and show good agreement with independently determined particle size characteristics (Table 1). It is interesting to note that particles from the microsuspension exhibit larger effective area than FA-Micronized particles possibly due to more favorable morphology (Figure 3 a) and Figure 4 a)).

**Table 2.** Effective particle size parameters determined during the dissolution experiments.

Substance	Loading $\mu$ g/mL	Effective Area $\text{cm}^2/\text{mg}$	Radius $\mu$ m
FA-Micronized	74	2.6 $\pm$ 0.1	8.9
FA-Micronized	106	3.8 $\pm$ 0.1	6.0
FA-Untreated	56	2.2 $\pm$ 0.1	10.6
FA-Untreated	112	1.8 $\pm$ 0.1	13.1
Microsuspension	50	7.9 $\pm$ 0.1	2.9
Microsuspension	100	7.4 $\pm$ 0.1	3.1

### In Situ Monitoring of API Release From Nanoparticles

Previously, *in situ* measurement of the concentration of free API being released from a nanoparticle formulation was not possible due to the complex effect of simultaneous scattering and absorption of UV radiation by nanoparticles. Figure 8 demonstrates that the shape of the second derivative spectra of a nanoparticle solution is different from the second derivative spectrum of Naproxen itself.

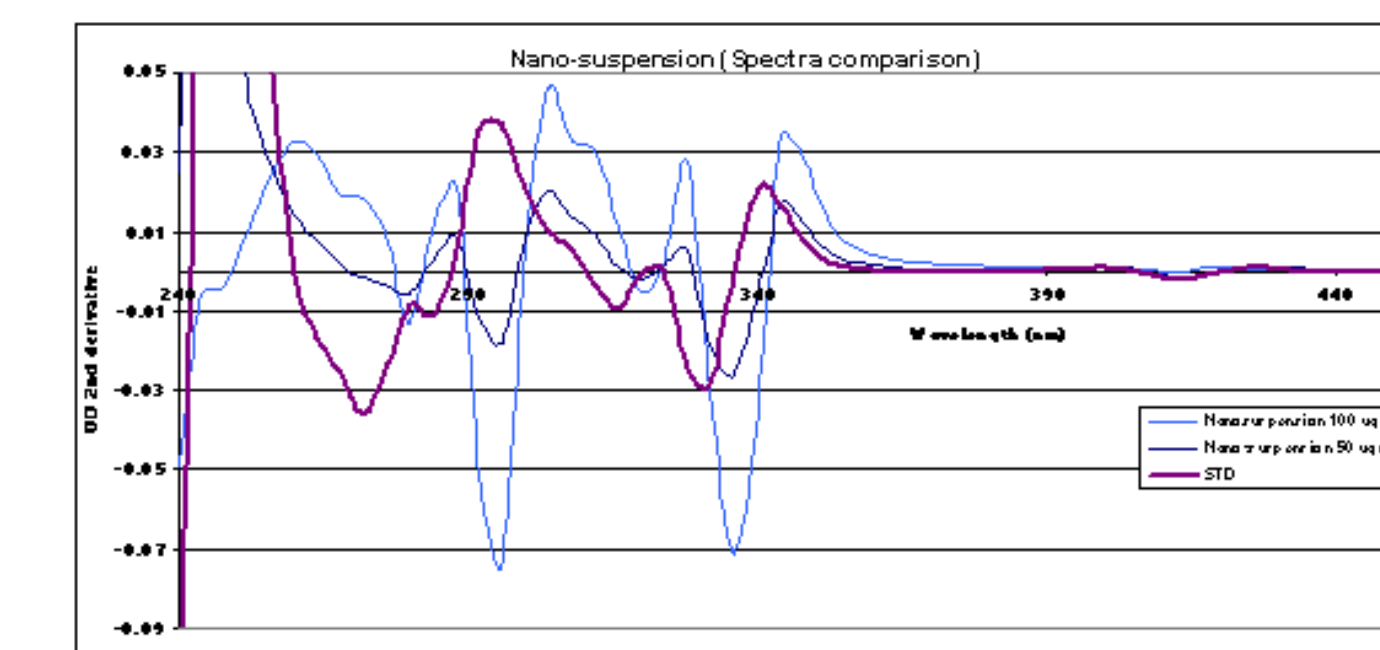


**Figure 8.** Second derivative spectra of dissolved Naproxen (STD, purple) and nanoparticles (50  $\mu$ g/mL dark blue and 100  $\mu$ g/mL light blue) in pH 1.2 USP buffer.

Figure 9 shows determination of the concentration of free (dissolved) Naproxen in equilibrium with its nanoparticles using ZIM. Zero intercepts of extrapolated lines indicate the equilibrium concentration of free API for 6 replicates.

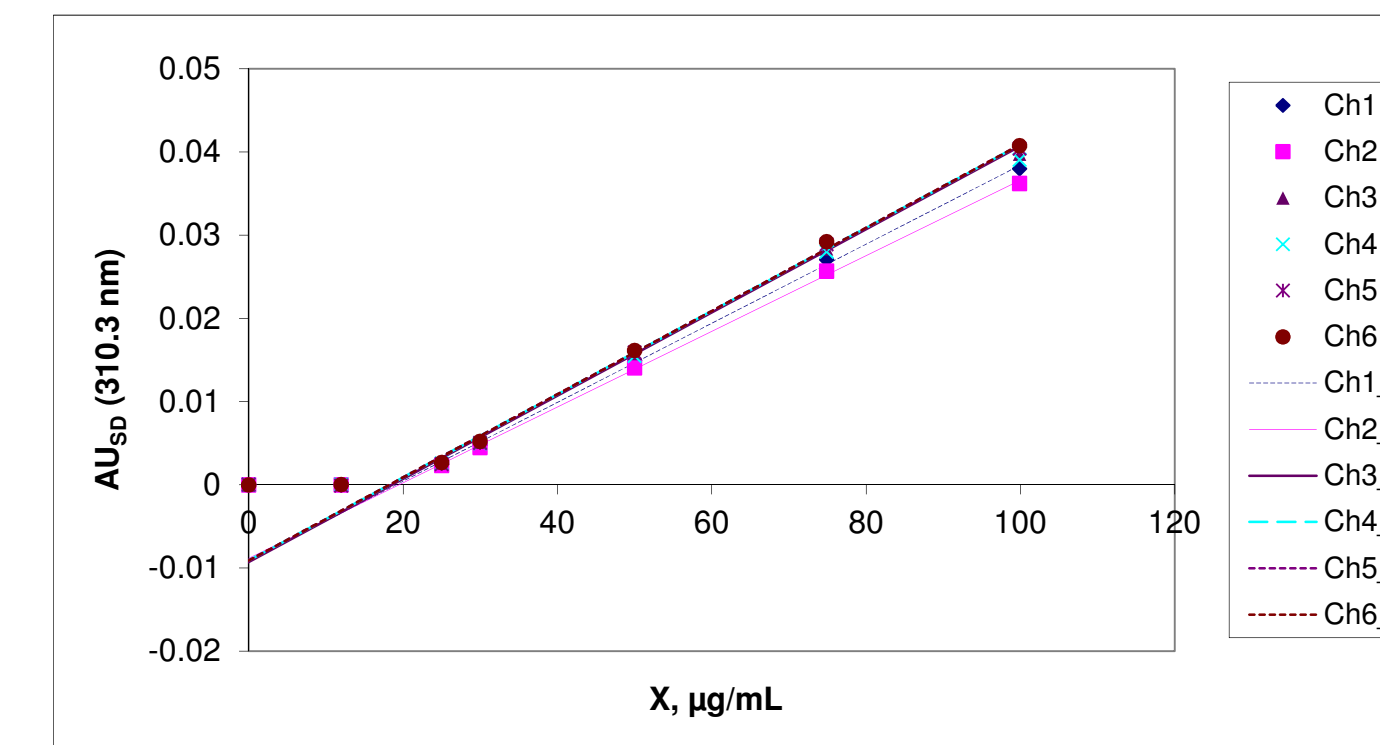


**Figure 9.** Plots of second derivative absorbance values (AU<sub>310.3</sub>) at 310.3 nm versus concentration of nanoparticles (X) in the solution in 6 vessels of the  $\mu$ DISS Profiler.

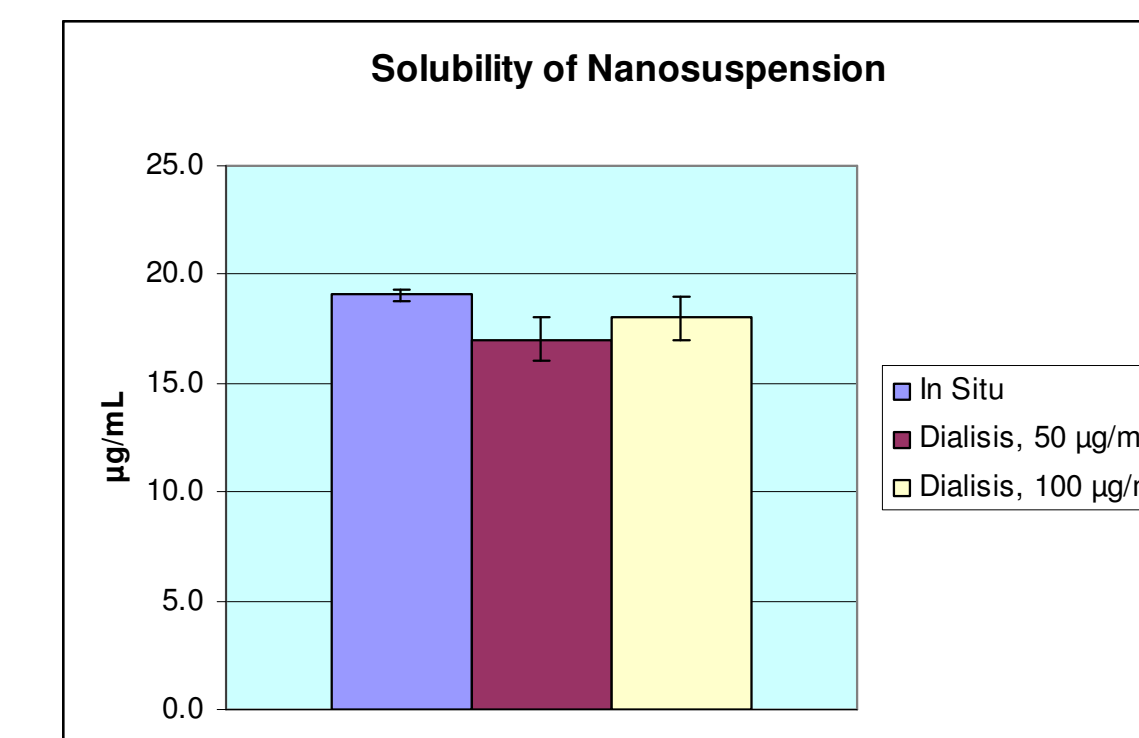


**Figure 10.** Solubility of Naproxen released from nanoparticles and measured *in situ* ( $\mu$ DISS Profiler) or using a 12 kDa dialysis membrane.

The *in situ* obtained value of 19.1  $\pm$  0.3  $\mu$ g/mL is in excellent agreement with values independently determined by equilibration through a dialysis membrane restrictive of nanoparticles, as shown in Figure 10.

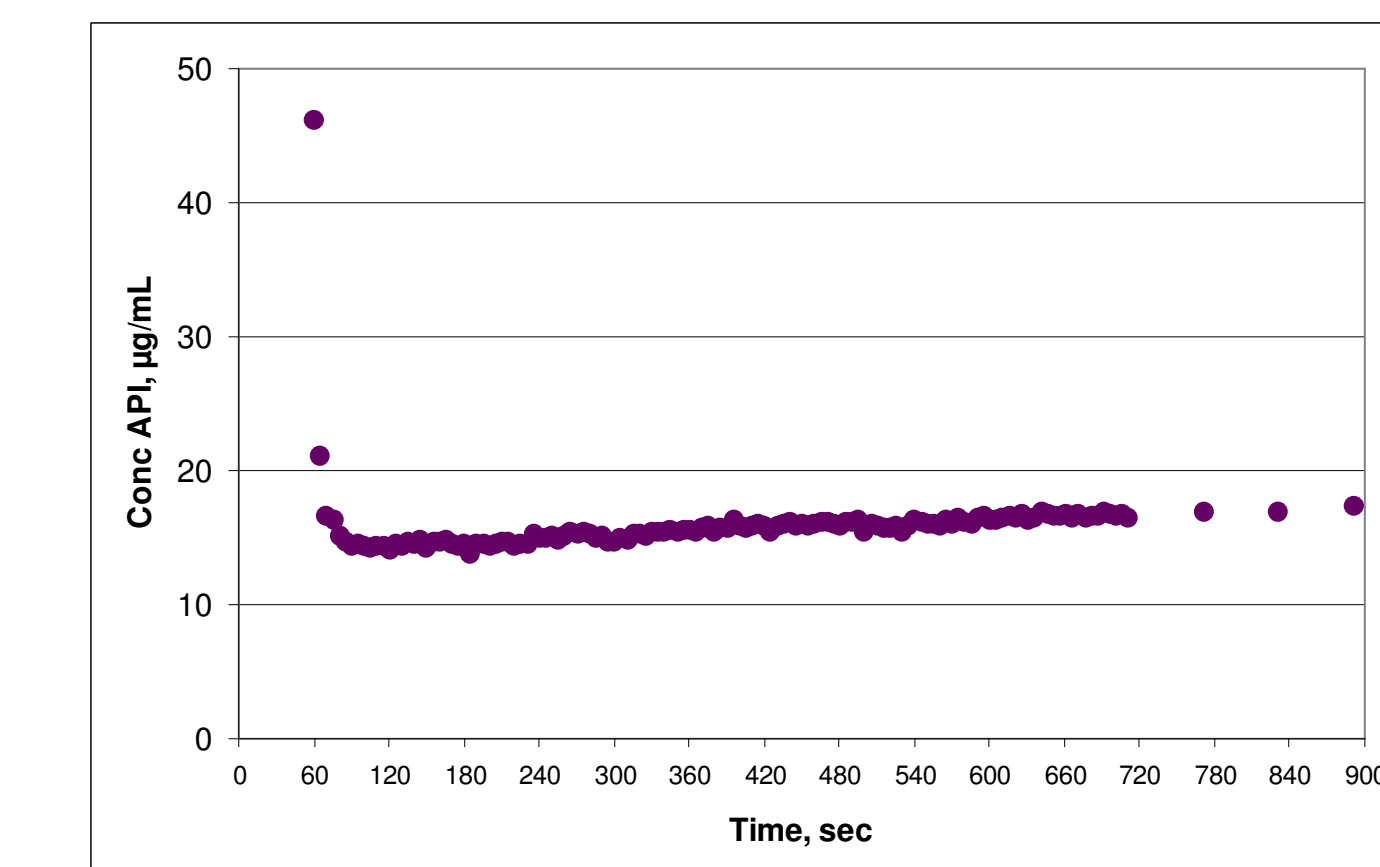


**Figure 11.** Monitoring of free Naproxen concentration after dispensing 10  $\mu$ L of a 100 mg/mL nanosuspension into pH 1.2 USP buffer.

Using the ZIM method it was also possible to monitor the concentration of free API after the nanosuspension is added to the aqueous buffer. Although the solubility of the nanoparticles was comparable to powders and the microsuspension particles, the equilibrium was reached, just seconds after mixing the nanosuspension with the buffer (Figure 11).

## CONCLUSIONS

A novel method has been developed for measuring in real time the concentration of free API released from nanoparticles without a need for particulate separation.

The solubility of Naproxen nanoparticles was found comparable to the solubility of powders while their dissolution/release behavior was qualitatively different.

It can be suggested that the extremely quick dissolution rate of nanoparticles may result in a preferable absorption rate for the API delivered as a nanosuspension.

The effective area of particles in the microsuspension appeared to be larger than that of FA-Micronized particles despite their similar particle size measured in the dry state.

Analysis of the dissolution profiles allowed estimation of particle size very comparable with independent measurements.